Solid Freeform Fabrication 2023: Proceedings of the 34th Annual International Solid Freeform Fabrication Symposium – An Additive Manufacturing Conference
Reviewed Paper

OUT-OF-PLANE MECHANICAL PROPERTIES OF ADDITIVELY MANUFACTURED FRACTAL REINFORCED STRUCTURES

Mario Martínez-Magallanes*, Enrique Cuan-Urquizo†, Erick Ramírez-Cedillo*, Armando Roman-Flores*.

*Tecnológico de Monterrey, School of Engineering and Sciences, Epigmenio González 500 Fracc. San Pablo, Querétaro 76130, México

†Tecnológico de Monterrey, Institute of Advanced Materials for Sustainable Manufacturing, Av. Eugenio Garza Sada 2501, Monterrey 64849, Mexico

Abstract

Architected materials are an emergent kind of materials that gain their physical properties from their rationally designed micro-structures. They are normally conformed by regular unit-cells repetition, but other variations, such as hierarchal, aperiodic, and graded arrangements have also been explored as well. Here we propose an approach consisting of using fractal geometry to control the mechanical response of the metamaterials. We designed a set of 11 different arrangements based on the self-filling Hilbert fractal, the set consisted of 3 different iteration orders at 3 different matching relative densities, and two other graded arrangements. The samples were fabricated using a Micro-LCD 3D-printer and tested under out-of-plane loads. The test was performed using a texturometer with a spherical probe impregnated with red paint to characterize the conformability of the samples. Force and displacement were recorded to compare the mechanical response of the samples against the fractal parameters and obtain the structure-property relation.

Keywords: *Fractal mechanical metamaterials, out-of-plane, Hilbert curve, conformability, additive manufacturing, LCD SLA.*

1. Introduction

Inspired by the sophisticated microarchitecture of natural porous materials, scientists have developed a new kind of materials known as metamaterials (MMs). MMs are man-made structured materials that gain their physical properties from their rationally designed microstructures rather than from their chemical composition alone [1]. The study of the geometry-property relationship in the field of MMs still has a long way to go and exploring the effects of topology and the influence of their geometrical parameters on the mechanical response of MMs remains essential to unveil the extraordinary capabilities of MMs.

Recent progress in manufacturing technologies, such as Computer Assisted Design (CAD) and Additive Manufacturing (AM) allow us to fabricate complex geometries that were very difficult to achieve with traditional manufacturing processes. This has triggered the interest of developing new MMs, intended to control different physical waves, including mechanical [2], acoustic [3], electromagnetic [4], and thermal [5] metamaterials. In the field of

mechanics, different non-conventional properties that are rarely found on common materials have been obtained from mechanical MMs design, including negative Poisson´s ratio [6,7], programmable shape morphing [8], non-linear responses [9], and improved strength-to-weight ratios [10].

Typically, MMs are conformed by periodic structures, which consists of single unit cell repetition to fill two or three-dimensional space. The unit-cells act as a continuum solid material, which allow us to track the structure-property relationship by studying the behavior of a single unit cell at the micro-scale within the effective response of the MM at the macro-scale. However, the range of properties that can be obtained with this approach is limited, therefore other geometrical variations have also been explored, including functionally graded structures [11], hierarchical arrangements [12], origami-like metamaterials [13], non-periodic [14] and fractal metamaterials [15].

Different fractal geometries have been already explored in the design of new MMs for controlling different physical waves, including acoustic, plasmonic and electromagnetic fractal MMs with enhanced properties. However, the use of fractal geometry on new MMs design in the field of mechanics has been slightly explored. For instance, Zhao et al. [16] investigated the uniaxial compression response of Nickel Titanium Menger sponge-like structures fabricated by AM via selective laser melting, showing super-elastic behaviors and matching properties of human cortical bones. Cheng et al. [17] incorporated Sierpinski triangle geometry into a triangular honeycomb to study the compressive response of TPU samples fabricated by AM and demonstrated an increase on compression strength and energy absorption performance on the iterated samples. Zhang et al. [18] explored the out-of-plane bending of chiral fractal beams that can be tuned through fractal iteration.

Applications pertaining the human body such as protective gear for athletes, prosthetic sockets, tissue engineering, and wearable devices, require considerations on comfort and functionality to avoid pain and malfunction. A large range of Young's moduli is required to solve the individual requirements from these applications. MMs have gain attention in this field due to their unique programmable properties and multifunctionality required to match the sophisticated anatomy and biomechanics of the human body. A variety of micro-architected geometries have demonstrated great functionalities in stretchability, extensibility, conformability, and out-of-plane deformation. Namely, Cho et al. [19] explored the effects of hierarchical cut patterns on the conformal wrapping response of a sheet around a nonzero Gauss curvature object for applications in stretchable devices and obtained custom properties and unique expandable behaviors. Pattinson et al. [20] explored the use of a hierarchical mesh with locally controlled mechanics to test conformability on a knee.

Hilbert fractal geometry has been previously used in the design of MMs to manipulate electromagnetic [21-23] and acoustic waves [24-26], but few explorations regarding the mechanical response of Hilbert MMs have been carried out, for instance Martínez-Magallanes et al. [27] investigated the behavior of Hilbert-based mechanical metamaterials under compression fabricated with thermoplastic polyurethane (TPU) via fused filament fabrication showing mechanical tuneability, and demonstrated an increase on stiffness

associated with the increase of Hilbert iterations. Exploring the out-of-plane properties of additively manufactured MMs present a great opportunity for research and innovation in sportive, medical, and wearable device technology. Fractal structures can offer remarkable conformability and customization, making them an ideal choice for these applications. Therefore, the objective of this work is to characterize the out-of-plane response of fractal reinforced plates and validate the feasibility of using fractal geometry as an alternative design tool to create novel mechanical metamaterials with adjustable out-of-plane response. Here, the Hilbert self-filling curve was selected as a first exploratory geometry since it can create complex structures by following simple rules from a Lyndenmayer system, this geometry tends to fill the unit square, which simplifies the sample design with different fractal iterations, also, the self-avoiding nature of the fractal may lead into better flexibility.

2. Materials and methods

We proposed an experimental test consisting of fractal reinforced thin plates subjected to out-of-plane loading. First, we show the proposed methodology to synthetize the fractal metamaterial. Then, we describe the AM process, parameters, and materials to fabricate the samples. Finally, we explain the experimental setup for the mechanical test.

Fractal metamaterial design

As shown in Figure 1a, we designed a set of I-shaped samples fractal reinforced matrices, all the reinforced plates have the same external dimensions and matrix thickness, also, three other non-reinforced plates with different thicknesses were designed to match the relative densities of the reinforced samples. For this work we selected the Hilbert self-filling fractal curve as our base reinforcement geometry and offsetted the curve to control the relative density through the thickness definition. We designed a set of samples consisting of three different iterations of the Hilbert self-filling fractal curve, N5, N4 and N3, and by adjusting the thickness t of the fractal curve we matched the samples reinforcement at three different relative densities, $\langle\rho\rangle = 0.3$, 0.45 and 0.6 (Figure 1b). Additionally, two other designs with combinations of N4 and N5 fractal iterations were created to obtain hybrid microstructures with a matching relative density $\langle\rho\rangle = 0.45$ (Figure 1c). The same design template can be applied to further explore the behavior of other complex geometries, including functionally graded structures, other self-filling curves and combinations with cellular structures.

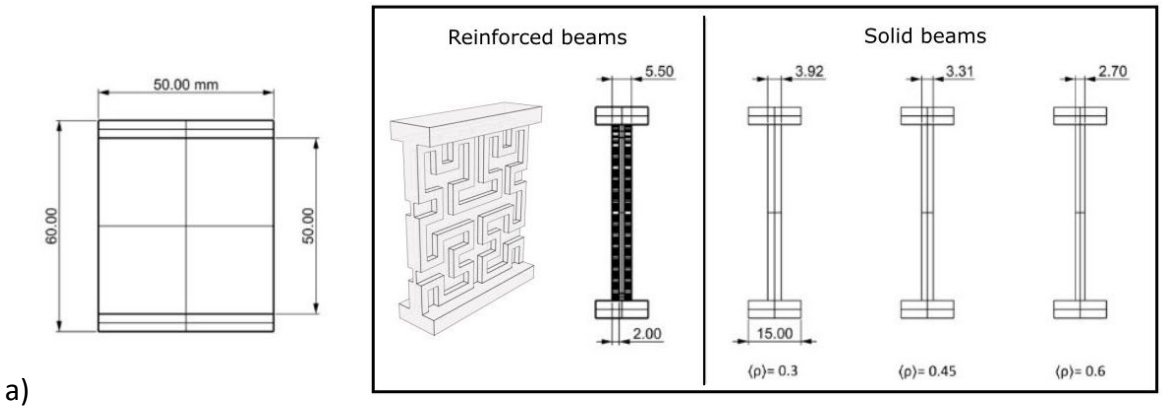

a)

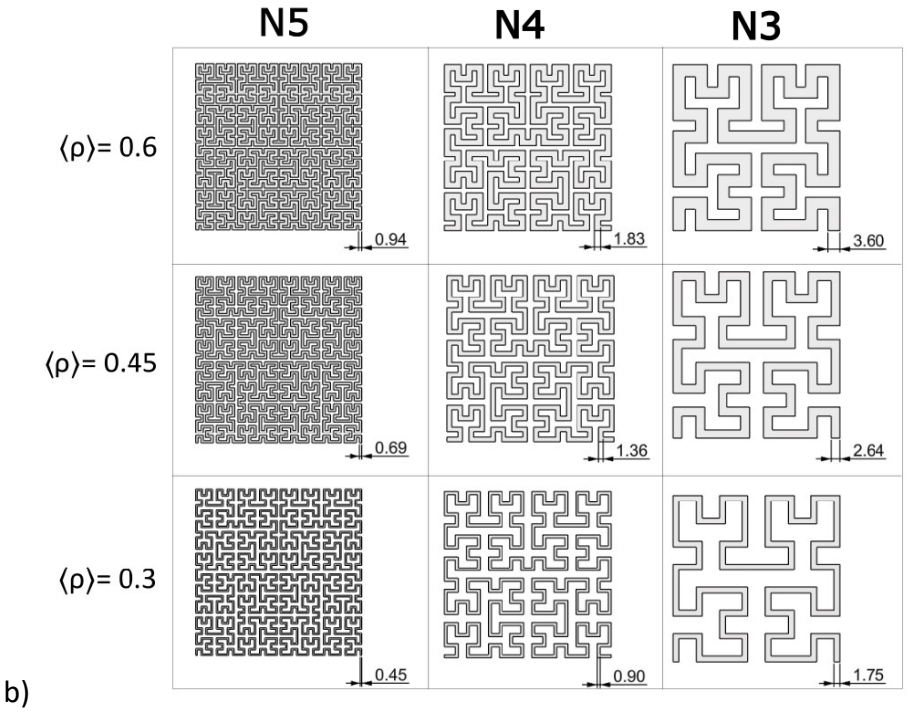

b)

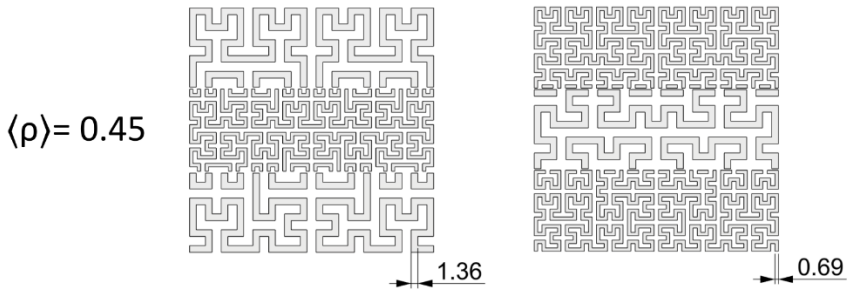

c)

Figure 1. Fractal reinforced thin plates design: a) I-shaped samples b) Hilbert reinforcements at matching relative densities c) Graded 1 and graded 2 Hilbert reinforcements. All the dimensions are in mm.

Additive Manufacturing of fractal metamaterials

All the designs were 3D modeled using Rhinoceros 6 CAD software, saved as .stl, sliced into a .gcode and fabricated with an Anycubic Mono X LCD resin printer, using Jamghe® Elastic Clear resin (Figure 2). A total of 42 samples consisting of 3 replicas of each design were fabricated using the same manufacturing parameters. All manufacturing parameters including layer height and printing speed are summarized Table 1. This resin is very flexible and can withstand large deformations before it brakes, it has a tensile modulus of 0.59 MPa, a tensile strength of 0.66 MPa, shore hardness 40-45 A, and density between 1.05 and 1.25 g/cm^3. After fabrication, the samples were cured using Isopropanol and subsequently dried.

Table 1. 3D printing parameters

Layer height	0.05-0.1 mm
Bottom layer count	4-6 layers
Exposure time	8-12 seconds
Bottom exposure time	60-90 seconds
Printing speed	30 mm/hour
Lifting height	5-7 mm

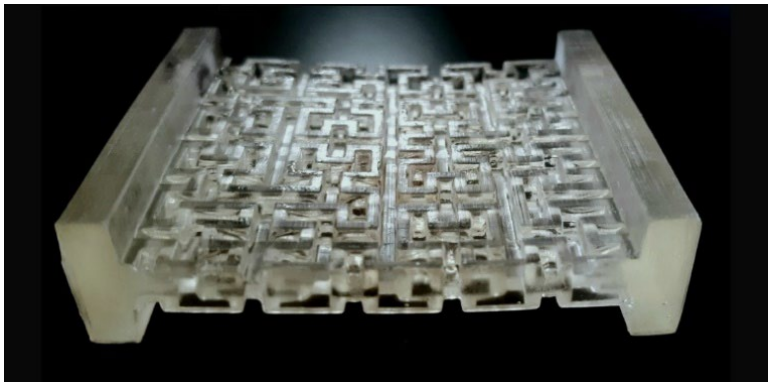

Figure 2. 3D printed Hilbert-reinforced plate.

Experimental setup

While most studies focus on the out-of-plane crushing behavior of honeycombs, studies on out-of-plane penetration are less common to observe, however this type of deformation may commonly occur. Therefore, we designed an experimental setup to test the out-of-plane stiffness of the samples. The samples were tested on a Perten TVT 6700 Texture Analyzer (PerkinElmer, Waltham, United States) with a 50kg load cell. The mechanical test was carried out by loading the samples in their out-of-plane direction using a 10 mm spherical probe 673110 at a test speed of 1mm/s, and a maximum displacement of 20 mm. As observed in Figure 3a, a custom case to lock up the samples on the heavy duty stand rig was designed and fabricated with an Ultimaker 3 FDM printer, using yellow Ultimaker PLA.

a) 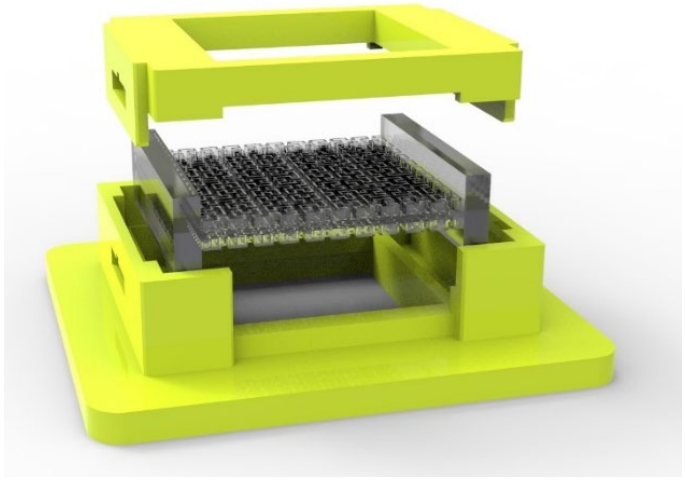 b) 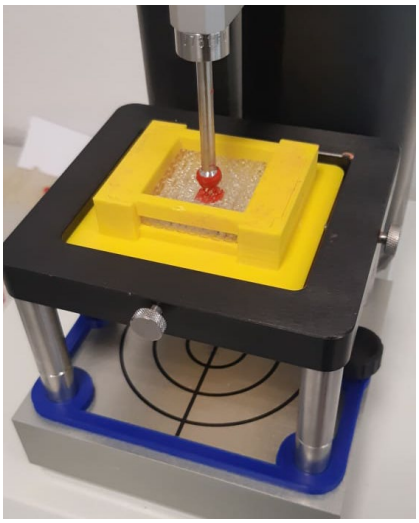

Figure 3. Out-of-plane experimental setup.

A photograph of the experimental setup is shown in Figure 3b. From the experimental test, Force $\boldsymbol{F}$ and displacement $\boldsymbol{\delta}$ were recorded at 200 points per second, using the TexCalc software and further processed in Excel and MATLAB. A very likely property to obtain for devices that will interact with the complex target surfaces is conformability, which refers to the ability of a surface to cover another one with high level of contact. From our experimental test we decided to study the load-conformability behavior of the samples by the spherical probe to study how the structure behaves under external loads as would happen in an application with complex target surface. This approach to measure the conformability of a geometry subjected to out-of-plane loads differs from others in literature, where the structures are not subjected to stress during their conformability characterization [28]. Therefore, we proposed to impregnate the spherical probe with red paint before each test and measure the resulting footprints to characterize the load-conformability behavior.

This experimental setup configuration was designed to obtain oval-like footprints, which let us characterize two different diameters, which makes the test more robust for asymmetric topologies. Figure 4 presents a photography of a sample after the experimental test impregned with the red paint showing the major and minor axes of the oval and characterized as D1 and D2. This approach can be easily replicated with other topologies to characterize their stiffness and conformability to obtain a further understanding on the out-of-plane behavior of micro-structured materials.

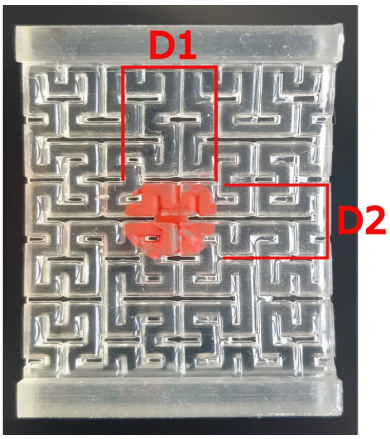

Figure 4. Footprint diameters definition

2. Results and discussion

LCD 3D printing of fractal reinforced plates

Table 2 shows the difference that we obtained between the CAD models and the 3D printed samples. The CAD model mass was calculated multiplying the total volume of each design by the materials density, here a density of 1.22 g/cm^3 was used to calculate the mass. The 3D printed samples were weighed with a digital weighing scale. For the solid plate designs, we obtained good accuracy between the printed and predicted masses, while for the reinforced plates notable discrepancies were found. As we can observe from Table 2, an increase on the actual mass occurred as we iterated the fractal curve, indicating a loss of resolution at small scales.

Table 2. CAD vs actual 3D printed masses.

	⟨ρ⟩= 0.3	**⟨ρ⟩= 0.3**		**⟨ρ⟩= 0.45**	**⟨ρ⟩= 0.45**		**⟨ρ⟩= 0.6**	**⟨ρ⟩= 0.6**	
Sample type	**CAD**	**Actual**	**Error %**	**CAD**	**Actual**	**Error %**	**CAD**	**Actual**	**Error %**
Solid plate	17.3 g	17.37 ± 0.03 g	0.4 %	19.3 g	19.32 ± 0.07 g	0.1 %	21.1 g	20.91 ± 0.14 g	0.9 %
Hilbert N3	17.3 g	19.13 ± 0.02 g	10.6 %	19.3 g	21.18 ± 0.07 g	9.7 %	21.1 g	22.96 ± 0.02 g	8.8 %
Hilbert N4	17.3 g	20.58 ± 0.17 g	19.0 %	19.3 g	22.95 ± 0.04 g	18.9 %	21.1 g	24.36 ± 0.14 g	15.4 %
Hilbert N5	17.3 g	22.89 ± 0.13 g	32.3 %	19.3 g	24.28 ± 0.14 g	25.8 %	21.1 g	25.24 ± 0.15 g	19.6 %
Hilbert GD1				19.3 g	22.89 ± 0.24 g	18.6 %			
Hilbert GD2				19.3 g	23.44 ± 0.02 g	21.5 %			

Out-of-plane force-displacement response

In this study, the out-of-plane mechanical behavior of fractal metamaterials is explored experimentally. The effects of the fractal iteration are presented in load-displacement curves (Figure 5) with the average values of each design arranged by relative density ⟨ρ⟩. We tested the samples at a maximum displacement of 17 mm. None of the samples fractured during the experimental tests.

From the plotted curves we can observe that the material does not obey Hooke´s law. Elastic resins as well as other elastomers present non-linearities, very large elastic regions and not well-defined plastic regions. All the samples exhibited rate-dependance behaviors, showing three main regions, an initial linear response, followed by an exponential phase and a final linear response.

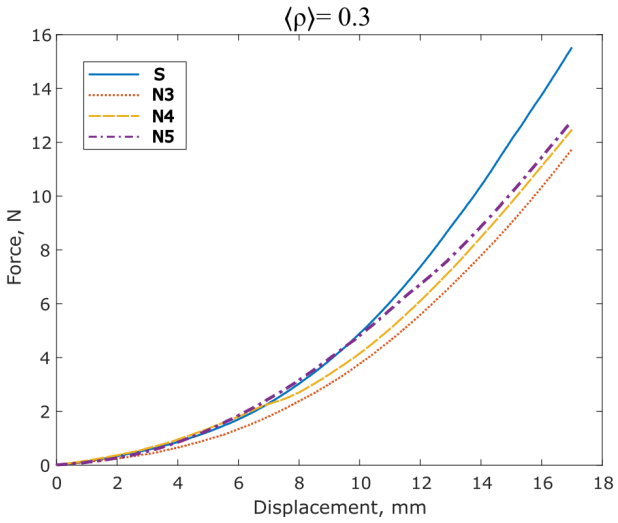

a)

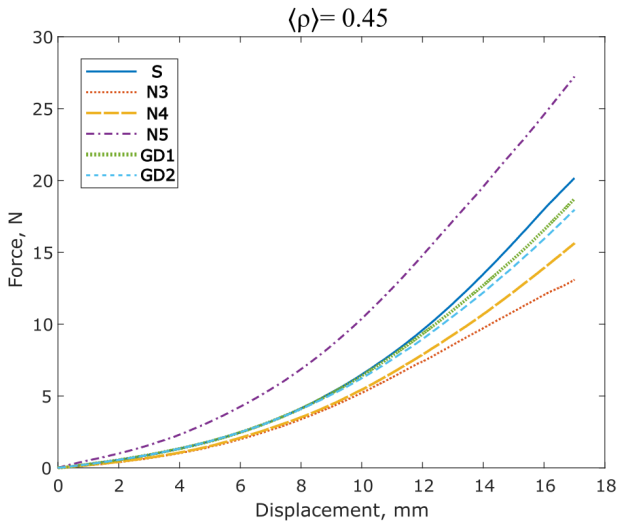

b)

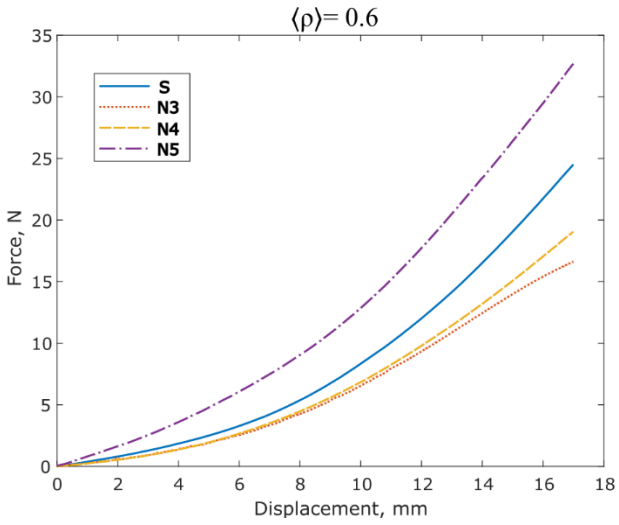

c)

Figure 5. Fractal iteration load-displacement plots at 3 different relative densities: a) Low relative density b) Medium relative density c) High relative density

The curves from Figure 5 show a tendency where the stiffness of the reinforced plates increases as we iterate the fractal curve, but these results are subjected to an error due to large deviations between the theoretical and actual masses. From Table 2, we observed that 4 samples resulted to have the best actual density $\langle\rho\rangle = 0.75$, 3 of consequent Hilbert iterations and 1 of the graded designs. Therefore, we compared the load-displacement curves of those 4 samples to validate if the increase on stiffness was related to the fractal iteration or to the mass deviations. Figure 6a shows the load-displacement curves from those 4 samples: Hilbert N3 at $\langle\rho\rangle = 0.6$, N4 at $\langle\rho\rangle = 0.45$, N5 at $\langle\rho\rangle = 0.3$ and GD1 at $\langle\rho\rangle = 0.45$.

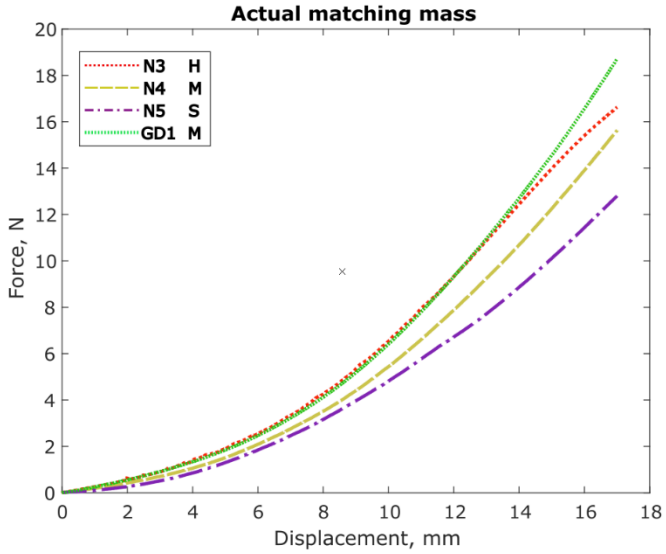

Figure 6. Actual matching density load-displacement curves.

By observing the influence of the geometry on the samples from Figure 6, there is an inverse tendency as the one observed in the plots from Figure 5, therefore the increase on stiffness from Figure 5 is mostly attributed to the actual mass discrepancies rather than from the fractal iterations. From the actual matching curves, we can observe that as we iterated the fractal curve, the sample became more flexible, at low and large displacement rates. Also, for the graded plate, an increase on stiffness occurred compared to its non-graded counterparts N4 and N5. From these curves, the stiffness was calculated from the linear regions at low and high displacement ranges.

The stiffness at the initial linear region, calculated from the start of the curve and up to $\delta = 4$ mm, as for the second region we delimited the slope in the displacement range from 11 to 15 mm. Table 3 shows the stiffness of the initial and second linear regions. From the first region, the Hilbert N3 configuration resulted the stiffest reinforced design with a difference of 5% with GD1, then the GD1 stiffness increased and resulted 9.7% stiffer than N3 at the second region. As for the fractal iteration we encountered an iteration-decrease response at both ranges, with a difference of 9.7% at low range and 10% at large range between N3 and N4, followed by a decrease of stiffness of 32.4% between N4 and N5 at low range and 29.6% at high range.

Table 3. Stiffness at low and high deformation ranges.

Sample type	Initial stiffness (N/mm)	Second region stiffness (N/mm)
Hilbert GD1	0.33	1.69
Hilbert N3	0.35	1.54
Hilbert N4	0.26	1.4
Hilbert N5	0.21	1.08

From Table 3 it was found that iterating the fractal geometry increases the flexibility of the structures, as reported by Zhang [18]. If we observe the fractal reinforcement geometry at the area where the load is being applied, we can observe that the Hilbert curve at fractal order N3 resulted in larger and thicker beam elements, making them more resistant to elastic deformation at both axes. As we iterate the curve, the curve becomes larger and the thickness needs to be reduced to about its half to match the relative density of the previous iteration, leading to thinner discontinuous elements and making the structure more flexible.

The GD1 configuration demonstrated enhanced performance and conformability. From analyzing the stiffness characterization presented in Table 3 it can be considered that when the stress caused by the spherical probe starts, the N5 elements that are concentrated in the middle of the sample have more participation against the load, making it flexible and conformal, then as the load increases the stress is partially relieved by the external Hilbert elements and causing an increase on stiffness at different stages. These results lead us to

further analyze topology combinations to enable larger tuneability and enhancement of the mechanical properties of reinforced plates with desired properties in specific locations.

Finally, to show the actual effects of geometry and relative density on stiffness, we plotted the initial stiffness from the additively manufactured samples with their actual relative density. Figure 7 shows the density-property relationship from the proposed structures.

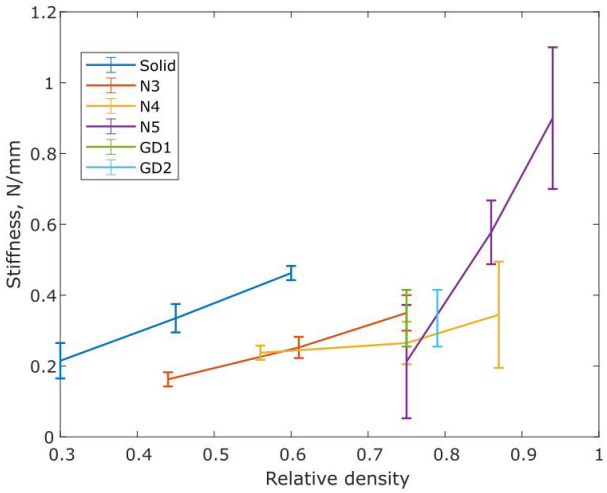

Figure 7. Actual density-stiffness relationship.

Out-of-plane load-conformability characterization

Due to the test setup and the geometry from our samples we obtained oval-like footprints. In Figure 8, the major and minor diameters were measured from the footprints to characterize the conformability of the sphere on the membranes.

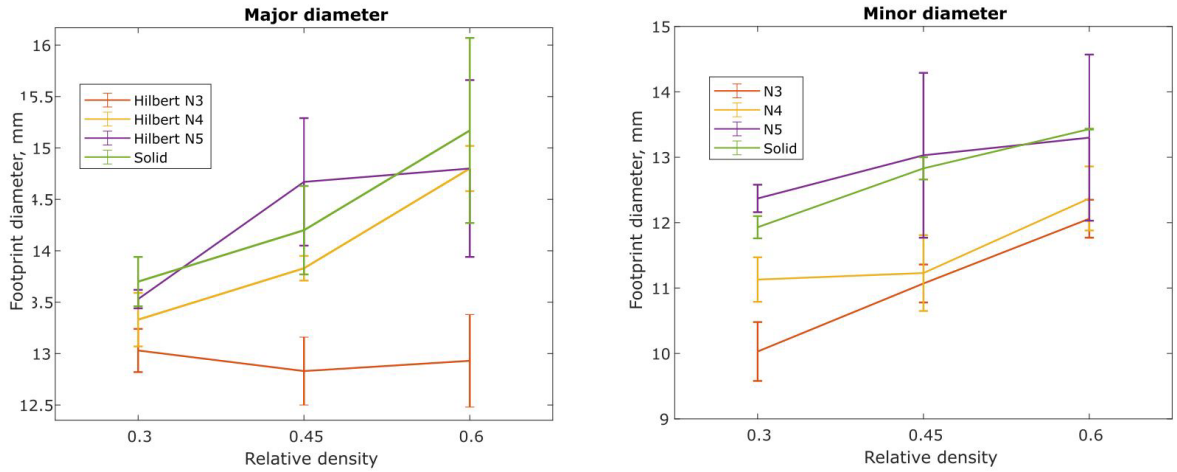

Figure 8. Major and minor footprint diameters.

The findings from Figure 8 show that for most cases, increasing the fractal order and/or the relative density also increased the conformability of the reinforced structures. At each

iteration the main elements of the structure are fractured into smaller copies of itself, making it more conformal at each step. Since the stress is mainly concentrated at the middle of the geometry and at the supports, not all the elements are contributing equally against the deformation.

Also, the Hilbert curve has only one line of reflexive symmetry, which will result in symmetric energy dissipation at the vertical axis but will present asymmetrical stress distribution from the horizontal axis. The fractal iterations are created by a combination of hierarchical translational and rotational symmetry, which leads to uneven stress distributions at each iteration. This kind of reflexive symmetry is observed in all the Hilbert designs, including the graded samples.

As for the solid samples a link between thickness and stiffness is also evident. Different behaviors were obtained for the solid plates compared to the reinforced plates, the solid sample footprint at $\langle\rho\rangle = 0.6$ resulted the largest at both axes, then for the samples at $\langle\rho\rangle = 0.45$ the Hilbert N5 design obtained the biggest footprint, finally, for the samples at $\langle\rho\rangle = 0.3$ the solid samples obtained the largest dimension at D1 but then the Hilbert N5 resulted larger at D2.

The results revealed a large range of tunable mechanical properties through fractal iteration and geometric parametrization. This experimental setup can be used to test other graded or non-graded topologies to characterize their out-of-plane behavior. Further exploration on diverse configurations from the experimental setup and Finite Element Analysis models may also be included in future work to assess the reliability from the test conditions, reduce the standard deviation and have more control over the fabrication variables. Nowadays there are numerous applications that require custom conformal materials, including stretchable electronic devices, helmets, prosthetic limb sockets and sport equipment. Therefore, further research on the out-of-plane mechanical properties of thin reinforced metamaterials must be addressed.

4. Conclusion

We used an LCD (Liquid Crystal Display) printer to fabricate different fractal mechanical metamaterial models and evaluate their out-of-plane behaviors. We defined three different relative densities and designed the samples to match those densities. We used the Hilbert fractal curve to design reinforced plates with three different iteration orders, also two graded designs with combinations of two levels of the Hilbert curve. The main findings of this research are:

- Fractal geometry was successfully used to fabricate meta-reinforced plates, this can be replicated with other topologies to further explore their out-of-plane behavior.
- The mechanical properties from the fractal metamaterials can be tuned by changing the fractal iteration order.
- The stiffness of the reinforced plates tends to decrease as the fractal order of the microstructure increases.

- The graded models show an increase on stiffness compared to their non-graded counterparts.
- It was found that as the thickness of the microstructures decreased, the samples actual mass increased.
- The sphere conformability increased as we iterated the fractal geometry.

5. Acknowledgments

We gratefully thank the support of the Consejo Nacional de Humanidades, Ciencias y Tecnología (CONAHCYT) Scholarship Program (scholarship number 779827) and 3D Factory MX for their support on this research. All this work has been done in the Metamaterials Lab at Tec de Mty, Querétaro, Mexico.

5. References

[1] Barchiesi, E., Spagnuolo, M., & Placidi, L. (2019). Mechanical metamaterials: a state of the art. *Mathematics and Mechanics of Solids*, *24*(1), 212-234.

[2] Jiang, Y., & Wang, Q. (2016). Highly-stretchable 3D-architected mechanical metamaterials. *Scientific reports*, *6*(1), 34147.

[3] Cummer, S. A., Christensen, J., & Alù, A. (2016). Controlling sound with acoustic metamaterials. *Nature Reviews Materials*, *1*(3), 1-13.

[4] Li, Y., Kita, S., Muñoz, P., Reshef, O., Vulis, D. I., Yin, M., ... & Mazur, E. (2015). On-chip zero-index metamaterials. *Nature Photonics*, *9*(11), 738-742.

[5] Sha, W., Xiao, M., Zhang, J., Ren, X., Zhu, Z., Zhang, Y., ... & Hu, R. (2021). Robustly printable freeform thermal metamaterials. *Nature communications*, *12*(1), 7228.

[6] Yang, L., Harrysson, O., West, H., & Cormier, D. (2015). Mechanical properties of 3D re-entrant honeycomb auxetic structures realized via additive manufacturing. *International Journal of Solids and Structures*, *69*, 475-490.

[7] Wang, H., Zhang, Y., Lin, W., & Qin, Q. H. (2020). A novel two-dimensional mechanical metamaterial with negative Poisson's ratio. *Computational Materials Science*, *171*, 109232.

[8] Florijn, B., Coulais, C., & van Hecke, M. (2014). Programmable mechanical metamaterials. *Physical review letters*, *113*(17), 175503.

[9] Rafsanjani, A., Akbarzadeh, A., & Pasini, D. (2015). Snapping mechanical metamaterials under tension. *Advanced Materials*, *27*(39), 5931-5935.

[10] Kobir, M. H., Liu, X., Yang, Y., & Jiang, F. (2022, June). Additive Manufacturing of Novel Beam Lattice Metamaterials With Hollow Cross-Sections Towards High Stiffness/Strength-to-Weight Ratio. In *International Manufacturing Science and Engineering Conference* (Vol. 85802, p. V001T01A027). American Society of Mechanical Engineers.

[11] Lira, C., & Scarpa, F. (2010). Transverse shear stiffness of thickness gradient honeycombs. *Composites Science and Technology*, *70*(6), 930-936.

[12] Meza, L. R., Zelhofer, A. J., Clarke, N., Mateos, A. J., Kochmann, D. M., & Greer, J. R. (2015). Resilient 3D hierarchical architected metamaterials. *Proceedings of the National Academy of Sciences*, *112*(37), 11502-11507.

[13] Zhai, Z., Wang, Y., & Jiang, H. (2018). Origami-inspired, on-demand deployable and collapsible mechanical metamaterials with tunable stiffness. *Proceedings of the National Academy of Sciences*, *115*(9), 2032-2037.

[14] Kumar, S., Tan, S., Zheng, L., & Kochmann, D. M. (2020). Inverse-designed spinodoid metamaterials. *npjComputational Materials*, *6*(1), 73.

[15] Sun, Y., Ye, W., Chen, Y., Fan, W., Feng, J., & Sareh, P. (2021, October). Geometric design classification of kirigami-inspired metastructures and metamaterials. In *Structures* (Vol. 33, pp. 3633-3643). Elsevier.

[16] Zhao, M., Qing, H., Wang, Y., Liang, J., Zhao, M., Geng, Y., ... & Lu, B. (2021). Superelastic behaviors of additively manufactured porous NiTi shape memory alloys designed with Menger sponge-like fractal structures. *Materials & Design*, *200*, 109448.

[17] Cheng, Q., Yin, J., Wen, J., & Yu, D. (2023). Mechanical properties of 3D-printed hierarchical structures based on Sierpinski triangles. *International Journal of Mechanical Sciences*, *247*, 108172.

[18] Zhang, Z., Scarpa, F., Bednarcyk, B. A., & Chen, Y. (2021). Harnessing fractal cuts to design robust lattice metamaterials for energy dissipation. *Additive Manufacturing*, *46*, 102126.

[19] Cho, Y., Shin, J. H., Costa, A., Kim, T. A., Kunin, V., Li, J., ... & Srolovitz, D. J. (2014). Engineering the shape and structure of materials by fractal cut. *Proceedings of the National Academy of Sciences*, *111*(49), 17390-17395.

[20] Pattinson, S. W., Huber, M. E., Kim, S., Lee, J., Grunsfeld, S., Roberts, R., ... & Hart, A. J. (2019). Additive manufacturing of biomechanically tailored meshes for compliant wearable and implantable devices. *Advanced Functional Materials*, *29*(32), 1901815.

[21] Elwi, T. A., Abdul Hassain, Z. A., & Tawfeeq, O. A. (2019). Hilbert metamaterial printed antenna based on organic substrates for energy harvesting. *IET Microwaves, Antennas & Propagation*, *13*(12), 2185-2192.

[22] Chen, R., Li, S., Gu, C., Anwar, S., Hou, B., & Lai, Y. (2014). Electromagnetic characteristics of Hilbert curve-based metamaterials. *Applied Physics A*, *117*, 445-450.

[23] Elwi, T. A., & Abdulqader, S. G. (2020). Further investigation on solant–rectenna-based flexible Hilbert-shaped metamaterials. *IET Nanodielectrics*, *3*(3), 88-93.

[24] Man, X., Liu, T., Xia, B., Luo, Z., Xie, L., & Liu, J. (2018). Space-coiling fractal metamaterial with multi-bandgaps on subwavelength scale. *Journal of Sound and Vibration*, *423*, 322-339.

[25] Man, X., Luo, Z., Liu, J., & Xia, B. (2019). Hilbert fractal acoustic metamaterials with negative mass density and bulk modulus on subwavelength scale. *Materials & design*, *180*, 107911.

[26] Comandini, G., Khodr, C., Ting, V. P., Azarpeyvand, M., & Scarpa, F. (2022). Sound absorption in Hilbert fractal and coiled acoustic metamaterials. *Applied Physics Letters*, *120*(6), 061902.

[27] Martínez-Magallanes, M., Cuan-Urquizo, E., Crespo-Sánchez, S. E., Valerga, A. P., Roman-Flores, A., Ramírez-Cedillo, E., & Treviño-Quintanilla, C. D. (2023). Hierarchical and fractal structured materials: Design, additive manufacturing and mechanical properties. *Proceedings of the Institution of Mechanical Engineers, Part L: Journal of Materials: Design and Applications*, *237*(3), 650-666.

[28] Yang, S., Choi, I. S., & Kamien, R. D. (2016). Design of super-conformable, foldable materials via fractal cuts and lattice kirigami. *Mrs Bulletin*, *41*(2), 130-138.